Scattering of H atoms on a Kr atom

Alberto Canali Fabio Mazza

I. The Numerov algorithm

In this exercise we are interested in solving numerically the stationary Schrödinger equation, in 1D or in the radial expression, for different potentials, namely the harmonic oscillator, for 1D and 3D, as a test for the correctness of the algorithm. We then apply the algorithm to a Lennard-Jones potential, in order to simulate a scattering process between a hydrogen atom and a target made of krypton, and calculate the phase shift resulting from the interaction between the atoms.

The heart of this program consists in the Numerov algorithm allows us to numerically solve second order differential equation in the form of:

$$\frac{d^2}{dx^2}y(x) + k^2(x)y(x) = S(x) \tag{1}$$

like the Schrödinger equation, which is a specific case for $S(x) = 0$.

The concept at the base of the algorithm is to use the three point formula for the second derivative of a function using $k^2(x)$ to calculate the correction given by the forth derivative applying again the three point formula:

$$\frac{y_{i+1} - 2y_i - y_{i-1}}{h^2} = y_i'' + \frac{h^2}{12}y_i^{iv} \tag{2}$$

$$y_i^{iv} = \frac{d^2}{dx^2}\left(-k^2(x_i)y(x_i) + S(x_i)\right) \tag{3}$$

where h is the uniform step of the discrete mesh. With some algebra and by substituting the second equation inside the first one we arrive to the final Numerov formula for the Schrödinger equation:

$$\begin{aligned} y_{i+1}\left(1 + \frac{h^2}{12}k_{i+1}^2\right) - y_i\left(2 - \frac{5h^2}{12}k_i^2\right) + \\ + y_{i+1}\left(1 + \frac{h^2}{12}k_{i+1}^2\right) = 0 \end{aligned} \tag{4}$$

$$k^2(r) = \frac{2m}{\hbar^2}\left(E - V(r)\right) - \frac{l(l+1)}{r^2} \tag{5}$$

having expressed the S.E. in radial form where $V(r)$ is the potential of the problem we are considering, E is the energy value that is being tested and the last term is the contribution of the angular momentum

In order to apply this algorithm to find the eigenstates we have first of all to implement the boundary condition to the solution of the equation. In particular we are interested in physical solutions and so we have to impose to the wave functions calculated to be square integrable; these kind of solutions are found for certain values of the energy $E_{n,l}$ that are the eigenvalues of the hamiltonian we are studying. To obtain this we have to impose to the solution we are building with Numerov to be zero at some r_{max} enough far away from the minimum of the potential. The best way to impose this condition is actually to match two solutions, one calculated starting from zero moving forward to r_{max} and one calculated from r_{max} moving backward (with an exponentially decaying boundary condition), imposing the equality of the logarithmic derivatives at the classical barrier of the potential. In order to calculate the forward solution we have to impose at least some points at $r = 0$ calculated knowing the behaviour of the wave function near zero. We impose a maximum difference between the logarithm derivatives and we apply the secant method for the values of the energy when we find a inversion of sign in the difference in order to find the eigenvalues of the energy. We also have to check that the cause of inversion is not given by the presence of a node in the forward solution.

A. 1D harmonic oscillator

We test the Numerov algorithm against a well known system: the harmonic oscillator. At first we study the hamiltonian of the 1D problem, considering the adimensional hamiltonian:

$$\mathcal{H} = \frac{1}{2}\frac{d^2}{dx^2} + \frac{1}{2}x^2 \tag{6}$$

of which the eigenstates and eigenvalues can be analytically calculated:

$$\begin{aligned} E_n &= n + \frac{1}{2} \\ \psi_n(x) &= \frac{1}{\sqrt{2^n n! \pi^{1/2}}} e^{-\frac{x^2}{2}} H_n(x) \end{aligned} \tag{7}$$

where $H_n(x)$ are the Hermite polynomials and $\omega = 1$, $\hbar = 1$, $m = 1$ are being used.

The data found using our code is collected in the following table where it is compared with the analytical values:

n	Theoretical	Numerical
0	0.5	0.499999998458
1	1.5	1.500000000058
2	2.5	2.499999999969
3	3.5	3.499999999979
4	4.5	4.500000000005

Table I: Comparison between the first five theoretical eigenvalues of the 1D harmonic oscillator and the data found applying the Numerov algorithm.

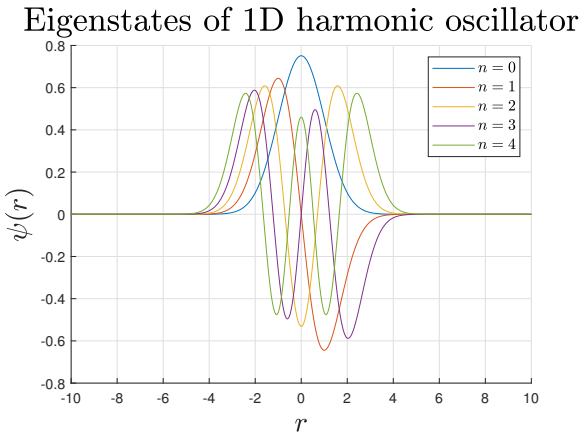

Figure 1: First five eigenfunctions of the 1D harmonic oscillator.

The numerical data are in good agreement with the theoretical ones. It is important to notice that in the code when we check the overlap of the forward and the backward solutions we can impose a maximum difference between the logarithmic derivatives of the wave functions, if this requirement is not satisfied the program iterates another time the calculation in order to improve the precision of the solution; here we set the precision to be 10^{-6} . In this way even if for quite short meshes, of 500 points, the values found are compatible to the theoretical values up to the fifth significant digit, while the numbers reported in Table 1 are calculated with a mesh long 150000 points. Working with this precision the program finds the eigenvalues with in the worst case seven iteration of the numerov algorithm.

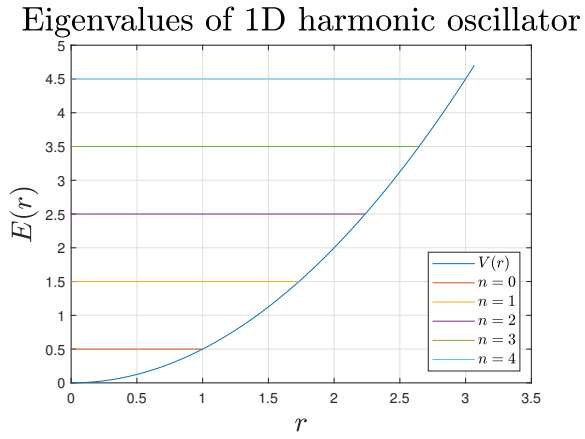

Figure 2: Eigenvalues of the harmonic oscillator calculated with the Numerov algorithm.

Contrary to the 3D harmonic oscillator and the scattering process the we will study later this case does not have a radial symmetry and so it is not possible to study the problem in the range from 0 to r_{max}, but we have to consider a larger interval going from $-r_{max}$ to r_{max} with the potential well centred in zero and using as boundary condition the asymptotic behaviour of the wavefunction at r_{max} and $-r_{max}$.

From the code we extract also the eigenvectors of the harmonic oscillator for the first five eigenvalues. The solution calculated by the algorithm in general are not normalized and this is one of the reasons we study the logarithmic derivatives, as it is independent from the normalization factors of the functions. The normalized eigenvectors and the eigenvalues are plotted in the following graphs:

II. 3D HARMONIC OSCILLATOR

The next step is to calculate the first eigenvalues and eigenstates of the 3D harmonic oscillator, considering the spherical symmetry of the potential and using spherical coordinates; the radial part of the hamiltonian studied then is:

$$H = \frac{1}{2}\frac{d^2}{dr^2} + \frac{1}{2}r^2 + \frac{l(l+1)}{r^2} \tag{8}$$

We apply again the Numerov algorithm for fixed values of l in order to find the spectrum up to a certain n_{max}.

As one should expect some of the eigenvalues found are degenerate as the eigenvalues predicted by the theory:

$$E_{nl} = 2n + l + \frac{3}{2} \tag{9}$$

The eigenvalues and the eigenstates are plotted in the following two figures for the first three values of l and the first three values of n.

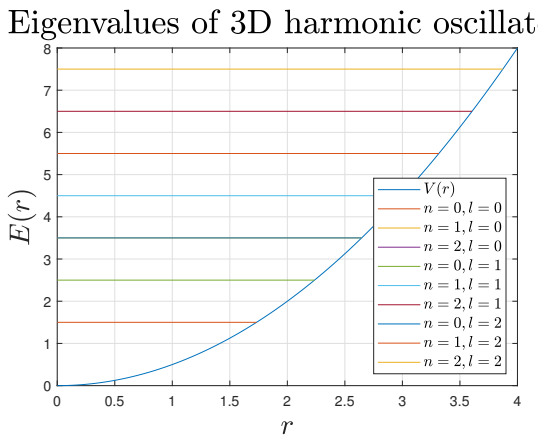

Figure 3: Eigenvalues of the 3D harmonic oscillator calculated with the Numerov algorithm.

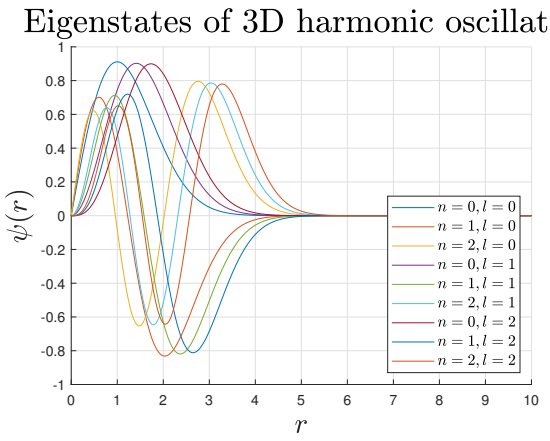

Figure 4: First nine eigenfunctions of the 3D harmonic oscillator.

One last thing to discuss before the scattering is the dependence of the eigenvalues on the length of the mesh. As said for the 1D case the program can find the eigenvalues with some degrees of accuracy even for quite short mesh having imposed to the program a fixed accuracy on the forward and backward solutions which translates to a certain accuracy on the values of energy. However we can still try to find a dependency of the values found on the number of points. We worked with a fixed r_{max} and so a change on the number of points of the mesh implies a longer interval h used in the numerov algorithm.

In the following graph we plot the ground state of the 3D harmonic oscillator as a function of the length of h, where we have fixed $r_{max} = 10$

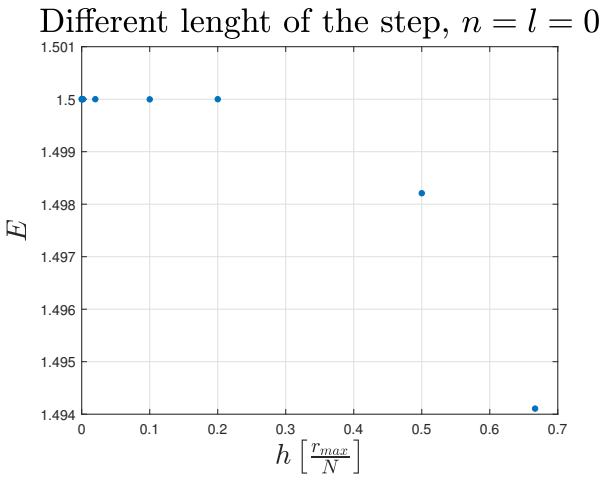

Figure 5

As it can be seen from the graph decreasing the length of the interval the accuracy on the energy increase converging to the exact value of the ground states. The worst value reported, that is about 1.4941, has been calculated using a mesh of only fifteen points. The eigenvalues of the harmonic oscillator can be considered almost independent on h, seeing that with a mesh of only 50 points the value calculated becomes: 1.4999999956 which can be considered quite good.

With Numerov being a fourth order method in h, we would expect bigger variations in the solutions, but these variations appear to be nullified by the process of derivative matching, which accepts the function with a predetermined tolerance.

III. Bessel Functions

In order to study the cross section of the $H - Kr$ scattering process we have to prepare a subroutine that calculates the Bessel functions with an iterative procedure following the relation:

$$s_{l+1} = \frac{2l+1}{x} s_l(x) - s_{l-1}(x) \tag{10}$$

where s_i stands both for the Bessel functions of the first kind j_i or the Bessel of the second kind n_l. In order to apply this recursive formula we have to know the $l = -1$ and $l = 0$ functions:

$$\begin{aligned} j_{-1}(x) &= \frac{\cos(x)}{x} \quad & j_0(x) &= \frac{\sin(x)}{x} \\ n_{-1}(x) &= \frac{\sin(x)}{x} \quad & n_0(x) &= -\frac{\cos(x)}{x} \end{aligned} \tag{11}$$

The function written in *C* is:

```
void fast_bessel(double x, double lmax, double *J)
{
    for (int l=1; l<lmax; l++)
        J[l+1] = ((2*l+1)/x) * J[l] - J[l-1];
}
```

where the function takes as input a vector with the two first term of the bessel function that we are interested in, already evaluated at the coordinate of interest.

	Wolfram	fast_bessel
j_0	0.841471	0.841471
j_1	0.301169	0.301169
j_2	0.062035	0.062035
n_0	−0.540302	−0.540302
n_1	−1.381773	−1.381773
n_2	−3.605018	−3.605018

Table II: Comparison between the first three spherical bessel functions, calculated both with our function and with Wolfram Alpha™ for $x = 1$.

As it can be notice the agreement between the values is perfect at least with this number of significant digits.

IV. Natural units for the scattering process

In order to solve the problem in units of the interatomic potential we start by computing the reduced mass μ of H and Kr, and then $\hbar/2\mu$, all in SI units. $\hbar/2\mu$ has the dimensions of an energy times a length squared, so the reduced constant is:

$$\left.\frac{\hbar}{2\mu}\right|_{\text{natural}} = \frac{\hbar/2\mu}{\varepsilon\sigma^2} = 0.035$$

with $\varepsilon = 5.9 \times 10^{-3}\ eV$ and $\sigma = 3.18$ Å.

V. Boundary conditions for the scattering process

By substituting $\exp\left[-(b/r)^5\right]$ into the radial Shrödinger equation it can be proven that it is a solution for $r \to 0$, with $b = \left(\frac{8\mu}{25\hbar}\right)^{\frac{1}{10}}$ in units of σ and ε.

In fact:

$$-\frac{\hbar^2}{2m}\frac{5b^5 e^{(-b/x)^5}(5b^5 - 6x^5)}{x^{12}} + 4\varepsilon\frac{\sigma^{12}}{x^{12}}e^{(-b/x)^5} -$$
$$-4\varepsilon\frac{\sigma^6}{x^6}e^{(-b/x)^5} + \frac{\hbar^2}{2m}\frac{l(l+1)}{x^2}e^{(-b/x)^5} = Ee^{(-b/x)^5}$$
$$-25b^{10}\frac{\hbar^2}{2m} + 4\varepsilon\sigma^{12} = 0 \Rightarrow b = \sqrt[10]{\frac{4\varepsilon\sigma^{12}}{25\hbar^2/2m}}$$

VI. Scattering solutions and phase-shifts

The solution near 0 defined at section V has to be used up to an r_{low} such that the Numerov algorithm starts to run sufficiently far from the potential divergence in 0. When checking the correctness of the program we decided euristically to provide the analytical wavefunction up to $r_{low} = 0.63$, where $V = 1000$.

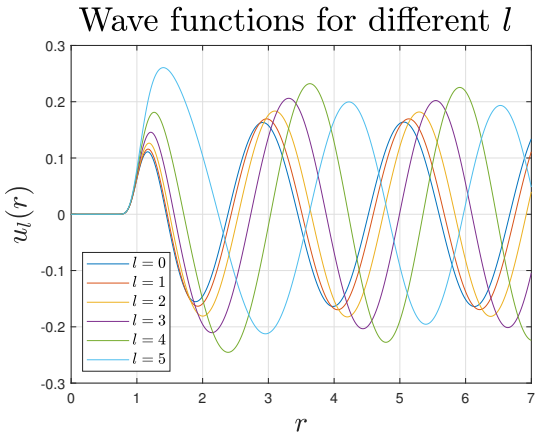

Figure 6: Scattering wavefunction at $E = 0.3\varepsilon$, for different values of l. The higher the angular momentum is, the higher is the distance of the atom to the quasibound state.

We then checked the results, specifically the total cross-section at an energy of $E = 0.3\varepsilon$, varying r_{low}.

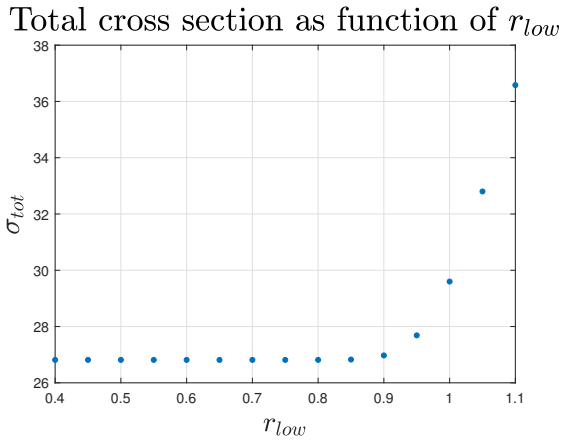

Figure 7

The trend of the cross-section meets our expectations: up to values of r_{low} where $V(r_{low})$ is higher than 0 by an amount of the order of ε, the result are fundamentally the same. For distances exceeding this point, the analytical approximation does not provide the correct wavefunction anymore. On the other hand, for points below ≈ 0.3, the algorithm breaks down producing NaNs.

The other parameters to check are the points r_1 and r_2 used to compute the phase shifts. We start by looking at the dependence of the total cross section on the distance between the two points, fixing r_2 near the farthest point of the grid.

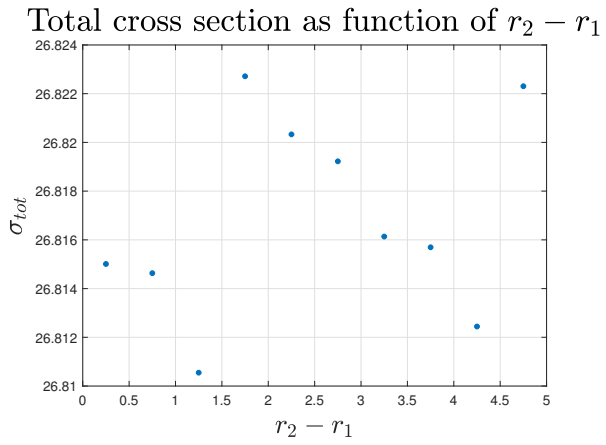

Figure 8

The dependence does not follow a clear trend, but is low nonetheless, with a maximum relative variation of 0.045%. We then choose to keep the distance $r_2 - r_1$ at a low value that produces an intermediate result, 0.75σ.

Then the dependence of σ_{tot} on the position of $r1$ and $r2$, varying both of them at a fixed distance, is calculated.

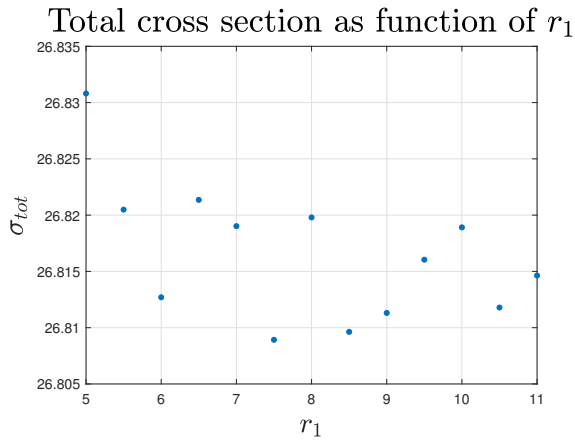

Figure 9

We see that for values near 5σ the cross-section seem to be more dispersed, although it does not completely converge for the distances reached by our mesh. Still, the relative difference is small enough for our purposes and we will assume the values at the maximum distance are the most accurate, thus choosing $r_1 = 11$ and $r_2 = 11.75$. These values could be lower, therefore reducing the computational time, but as will be seen in the next section, at higher energies contributions from higher values of l become relevant, and for these contributions the non-sinusoidal part of the wavefunction extends farther.

VII. Comparison with the experimental cross-sections

By repeating the calculation of the cross section for different kinetic energies we obtained the curves shown in figure 10 and 11.

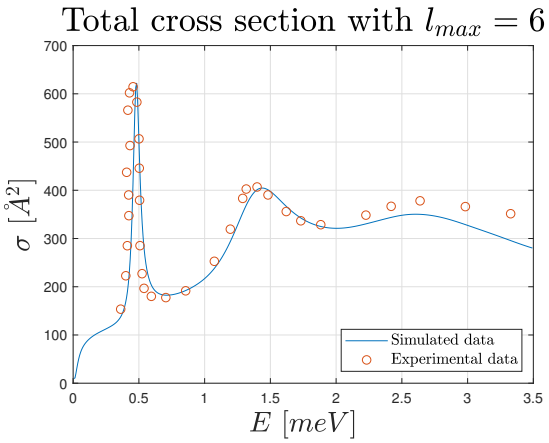

Figure 10: Comparison between the experimental data and the data obtained numerically taking in account contribution for max $l = 6$.

Comparing our results with the ones provided in the Toennies, Welz and Wolf paper, we can see that at lower energies there is substantial agreement, except for a global shift of the curve. This could be caused by a bad printing or a bad digitalization of the curve.

At higher energies our values underestimate those observed in the experiment, but this can be fixed by considering also higher values of the momentum.

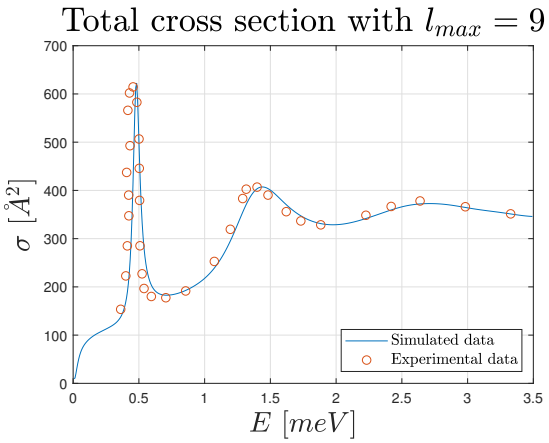

Figure 11: Comparison between the experimental data and the data obtained numerically taking in account contribution for max $l = 9$

Indeed by extending l up to 9 the experimental and theoretical values align even at higher energies.

In order to see how the different contribute to the cross section we plotted their contributions, given by $(2l+1)\sin^2(\delta_l)$.

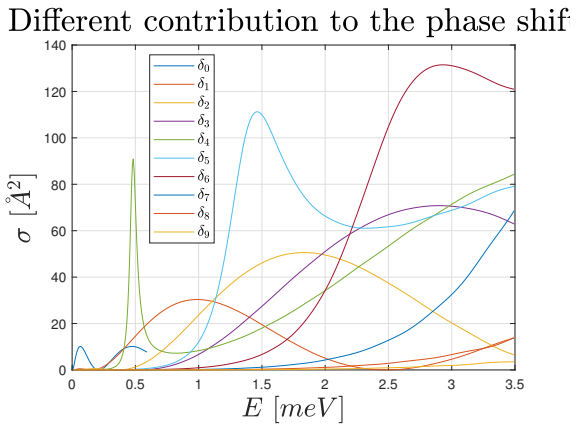

Figure 12: Different contribution to the cross section for different l

As can be seen, as the orbital angular momentum contribution gets higher, the energy of its maximum contribution gets higher. At the lowest energies the peaks are sharper, while at higher energy the discrete nature of the angular momentum begins having smaller effects and the cross section could be calculated even by a classical model.